

Lead-resistance effects in a constant voltage anemometer

Geneviève Comte-Bellot^{a)}

Centre Acoustique, LMFA, Ecole Centrale de Lyon, 69134 Ecully, France

Julien Weiss

Department of Mechanical Engineering and Material Sciences, Duke University, Durham, North Carolina 27708

Jean-Christophe Béra

Centre Acoustique, LMFA, Ecole Centrale de Lyon, 69134 Ecully, France

(Received 28 July 2003; accepted 29 March 2004; published online 24 May 2004)

Two effects of the lead resistances connecting the hot wire to a constant voltage anemometer (CVA) were analyzed and tested: one concerns the change in the sensitivity coefficient relating the anemometer output to velocity or temperature fluctuations, and the other the time constant of the hot wire determined by an *in situ* square-wave test technique. Small perturbations were assumed in both cases. The CVA output sensitivity was found to be reduced and the time constant increased with the lead resistance. Explicit formulas which involve the lead resistance, the cold wire resistance, and the wire overheat, as well as some characteristics of the CVA circuit, were established to take into account these effects. In the ranges tested, each effect can individually introduce as much as 10% error. Product of the two governs the overall response for the CVA. However, because the two effects change in opposite directions, interestingly, variation in the net response from their product is minimized. This feature may be very useful for many engineering applications of the CVA. Results of experiments conducted with the CVA in a subsonic jet are presented. They confirm the analysis and also establish that accurate measurements can be performed even with a large ratio of lead resistance to hot-wire resistance by applying the correction formulas developed with the analysis. Results from earlier experiments in a supersonic boundary layer also are presented.

© 2004 American Institute of Physics. [DOI: 10.1063/1.1753676]

I. INTRODUCTION

The constant voltage anemometer (CVA) is a technique pioneered and developed by Sarma.^{1,2} It presents several attractive qualities which are stability, low noise, and large bandwidth. Several improvements were later added to the initial setup, such as the software correction of the wire thermal lag by Sarma, Comte-Bellot, and Faure³ to insure constant bandwidth at a selected compensation setting, or the remote control of the instrument by Sarma and Lankes⁴ for flight applications. The possibility of quickly changing the wire overheat was also demonstrated by Sarma and Comte-Bellot⁵ as well as CVA applications with ambient temperature drifts without the need for any additional hot wire, unlike the constant temperature anemometer (CTA).⁶ This simplification was, for example, employed by Truzzi, Sarma, and Chokani⁷ in synthetic-jet studies. The large bandwidth feature of the CVA was used in several investigations in high-speed flows, such as turbulence measurements in supersonic boundary layers by Comte-Bellot and Sarma⁸ or Weiss *et al.*,⁹ and stability of hypersonic boundary layers over flared cones by Lachowicz, Chokani, and Wilkinson¹⁰ and

Reimann, Chokani, and Sarma.¹¹ Stepping of overheats in the CVA was developed by Norris and Chokani¹² for experiments in a shock wind tunnel.

Figure 1 shows a schematic diagram of the CVA circuit with its internal compensation circuit for the wire thermal lag and also the lead which connects the sensor to the anemometer input. The possible effect of the lead resistance was only recently considered. It was indeed easier to work on the wire alone, as done by Comte-Bellot¹³ when establishing explicit expressions for the sensitivity coefficients of the wire to either velocity or temperature changes, and expressions for the time constant of the wire. With the square-wave technique developed by Sarma² for *in situ* time constant measurement, the value obtained will be with the lead resistance.

The concern regarding the lead-resistance effect on sensitivity coefficient appeared first in Bailly and Comte-Bellot.¹⁴ Use of the correction factor they developed was attempted by Weiss *et al.*,⁹ but was not fully satisfactory. It gave too large turbulence intensities due to only partial corrections applied for the effect of lead resistance on the sensitivity, without the associated corrections for the time constants.

For the sensitivity coefficient to velocity or temperature fluctuations, *in situ* calibrations can often provide adequate solution to the problem. This will be easy in subsonic flows: for a jet, one can use the potential core, for a boundary layer, the external free stream. In both cases, turbulence levels are

^{a)}Author to whom correspondence should be addressed; electronic mail: genevieve.comte-bellot@wanadoo.fr

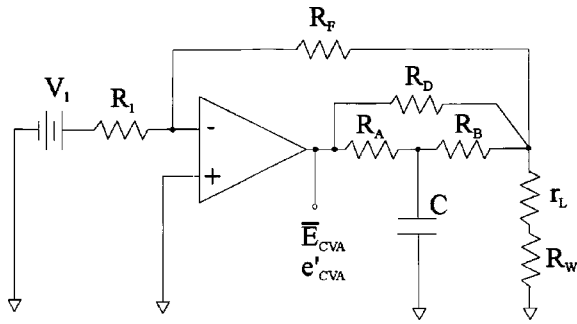


FIG. 1. Schematic diagram of the CVA circuit.

low, permitting fast and accurate calibration curves to be acquired. However, the problem becomes complicated in supersonic flows where special wind tunnels¹⁵ have to be used in order to adjust every one of the needed parameters (temperature, pressure, Reynolds number, and Mach number). The straightforward expressions¹³ obtained for the wire alone were therefore preferred, for example, in Comte-Bellot and Sarma,⁸ Reimann, Chokani, and Sarma,¹¹ or Ito *et al.*¹⁶

For the time-constant values, the lead effect has not been examined so far. The usual method of operation of the CVA is to record the “raw data” with a fixed electronic hardware compensation setting not necessarily equal to the actual hot-wire time constant. CVA is provided with diagnostic outputs that enable measurements of *in situ* hot-wire time constant and overheat. Using *in situ* measured hot-wire time constant and overheat, accurate perturbation quantities can be obtained through postprocessing.^{3,8} Since the wire time constant is measured *in situ*, it necessarily involves the connecting cable, whereas time constant for the wire alone is needed for perturbation calculations. The details of obtaining the time constant of the hot wire alone by correcting the measured time constant for the cable resistance is presented through analysis and tests in the following sections.

The article is organized as follows. The effect of the lead resistance on the CVA output response to velocity and temperature fluctuations is considered in Sec. II. An approach based on the sensitivity coefficients, with and without the lead resistance, permits the correction factor to be expressed in terms of its cold resistance, its overheat, and the lead resistance. Necessary parameters of the CVA circuit are also included. The lead resistance effect on the wire time constant is analyzed in Sec. III, and an explicit correction factor is derived. Section IV presents the experimental validations performed in a subsonic jet. Section V presents the improvement in results when both the corrections are applied for tests in a supersonic boundary layer.

II. CVA RESPONSE TO VELOCITY AND TEMPERATURE CHANGES WITH LEAD RESISTANCE

The CVA governing equations are available in Sarma²

$$V_s = \left[1 + \frac{R_2}{R_F} + \frac{R_2}{R_w + r_L} \right] V_w, \quad (1)$$

$$V_w = I_w (R_w + r_L) = \text{a constant.} \quad (2)$$

R_w is the resistance of the heated hot wire alone, I_w the current through the wire and the leads, r_L the lead resistance, and R_2 and R_F are resistances in the CVA circuit (see Fig. 1, $R_2 = R_A + R_B$, $R_D \gg R_2$). V_w is the voltage kept constant by the CVA circuit, it is applied across the wire and its lead resistance. King’s law, which conveniently represents the cooling of a long wire by forced convection, is also used to relate the terms as

$$\frac{R_w I_w^2}{R_w - R_a} = A + B \sqrt{U}. \quad (3)$$

R_a is the resistance of the unheated wire at ambient temperature, U is the velocity normal to the wire, and A and B are the usual “constants” depending on the wire which is used.^{13,17}

For small velocity perturbations, with primes denoting fluctuations and overbars the mean values, the log derivatives of Eqs. (1)–(3) give

$$\frac{v'_s}{\bar{V}_s} = - \frac{1}{1 + \frac{R_2}{R_F} + \frac{R_2}{\bar{R}_w + r_L}} \frac{R_2}{(\bar{R}_w + r_L)^2} r'_w, \quad (4)$$

$$\frac{i'_w}{\bar{I}_w} + \frac{r'_w}{\bar{R}_w + r_L} = 0, \quad (5)$$

$$\frac{r'_w}{\bar{R}_w} + 2 \frac{i'_w}{\bar{I}_w} - \frac{r'_w}{\bar{R}_w - R_a} = \frac{1}{2} \frac{B u'}{(A + B \sqrt{\bar{U}}) \sqrt{\bar{U}}}. \quad (6)$$

Substituting i'_w from Eq. (5) into Eq. (6) and eliminating r'_w between the resulting equation and Eq. (4) give

$$\frac{v'_s}{\bar{V}_s} = \frac{1}{1 + \left(1 + \frac{r_L}{\bar{R}_w} \right) \left(\frac{\bar{R}_w}{R_2} + \frac{\bar{R}_w}{R_F} \right)} \times \frac{1}{1 + \frac{r_L}{\bar{R}_w(1 + 2\bar{a}_w)}} \frac{\bar{a}_w}{1 + 2\bar{a}_w} \frac{1}{2} \frac{B \sqrt{\bar{U}}}{A + B \sqrt{\bar{U}}} \frac{u'}{\bar{U}}, \quad (7)$$

where \bar{a}_w is the mean wire overheat, $(\bar{R}_w - R_a)/R_a$.

In the CVA prototype, the V_s output is filtered with a 670 kHz Butterworth fourth order filter and at a hardware compensation setting $TC = 0.10$ ms, the system yields a 470 kHz bandwidth.⁸ This output voltage after the filter is used in the measurements, and will be represented here by \bar{E}_{CVA} for the mean value and e'_{CVA} for the fluctuation. At frequencies below the cut-off, the notations \bar{E}_{CVA} and e'_{CVA} can then be used in place of \bar{V}_s , and v'_s , and Eq. (7) can be rewritten as follows:

$$\frac{e'_{CVA}}{\bar{E}_{CVA}} = \tilde{S}_u^{CVA} \frac{u'}{\bar{U}} \quad (8)$$

with

\tilde{S}_u^{CVA} (for CVA output with lead resistance included)

$$= LS \cdot S_u^{CVA} \text{ (hot wire alone),} \quad (9)$$

and

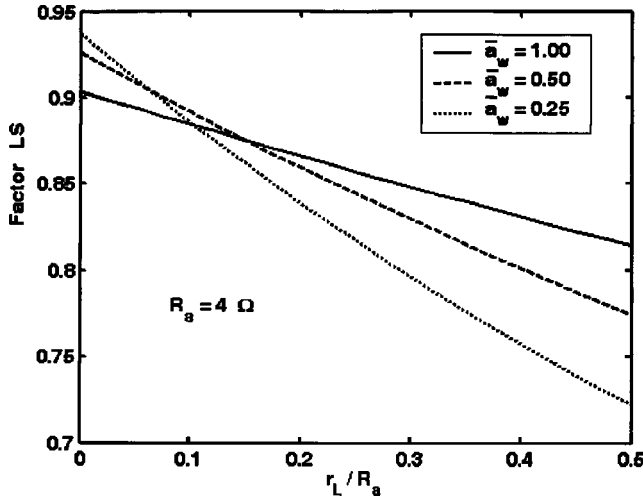


FIG. 2. Effect of the lead resistance r_L on the CVA sensitivity coefficient to velocity fluctuations. Factor LS is given by Eq. (10). Three hot-wire overheats \bar{a}_w are considered, and the cold wire resistance is $R_a = 4 \Omega$. The curves do not begin at unity for $r_L = 0$, because of the effect of resistances R_2 and R_F in the CVA circuit.

$$LS = \frac{1}{1 + \left(\frac{R_a}{R_2} + \frac{R_a}{R_F} \right) \left(1 + \bar{a}_w + \frac{r_L}{R_a} \right)} \times \frac{1}{1 + \frac{r_L}{R_a(1 + \bar{a}_w)(1 + 2\bar{a}_w)}}. \quad (10)$$

S_u^{CVA} is the sensitivity coefficient of the wire alone to velocity fluctuations, already established¹³:

$$S_u^{\text{CVA}}(\text{hot wire alone}) = \frac{\bar{a}_w}{2(1 + 2\bar{a}_w)} \frac{B\sqrt{\bar{U}}}{A + B\sqrt{\bar{U}}}. \quad (11)$$

Equation (10) shows the explicit relationship for the correction factor LS in terms of the cold resistance of the wire R_a , the mean hot-wire overheat \bar{a}_w , and the lead-resistance r_L . Figure 2 illustrates the variation of LS vs r_L/R_a , for several values of \bar{a}_w . The correction factor LS is always smaller than unity. For example, $LS \approx 0.85$ for $r_L/R_a \approx 0.25$ and $\bar{a}_w \approx 1$. Two circuit elements of the CVA, the resistances R_2 and R_F , are also included. Their typical values are $R_2 \approx 100 \Omega$, $R_F \approx 300 \Omega$, having minor influence on LS .

A similar derivation can be obtained for the sensitivity coefficient of the CVA for fluid temperature fluctuations, using King's law response to R_a :

$$\begin{aligned} \tilde{S}_{\theta_a}^{\text{CVA}} & (\text{for CVA output with lead resistance included}) \\ &= LS \cdot S_{\theta_a}^{\text{CVA}}(\text{wire alone}) \end{aligned} \quad (12)$$

with the LS factor again given by Eq. (10), and for the hot wire alone¹³

$$S_{\theta_a}^{\text{CVA}} = - \frac{1}{1 + 2\bar{a}_w} \chi \bar{T}_a [1 - \chi(\bar{T}_a - T_0)], \quad (13)$$

where χ is the linear temperature coefficient of resistance, \bar{T}_a the mean fluid temperature, and T_0 a reference temperature.

III. TIME CONSTANT WITH THE LEAD RESISTANCE

When heat losses due to conduction to the prongs are neglected, the dynamic response of the real hot wire, of mass m_w and specific heat c_w is given by¹⁸

$$\frac{m_w c_w}{R_a \chi} \frac{dR_w}{dt} = R_w I_w^2 - (R_w - R_a)(A + B\sqrt{U}) \quad (14)$$

and that of an ideal hot wire which would always be in equilibrium relative to external parameters

$$0 = R_w^* I_w^{*2} - (R_w^* - R_a)(A + B\sqrt{U}). \quad (15)$$

The CVA circuit imposes

$$(R_w + r_L)I_w = (R_w^* + r_L)I_w^* = \text{a constant} = V_w, \quad (16)$$

where R_w is the resistance of the real hot wire, R_w^* the resistance of the ideal wire, I_w the current in the real wire, and I_w^* the current in the ideal wire.

Combining Eqs. (14)–(16) gives

$$\frac{1}{V_w^2} \frac{m_w c_w}{R_a \chi} \frac{dR_w}{dt} = \frac{R_w}{(R_w + r_L)^2} - \frac{(R_w - R_a)}{(R_w^* - R_a)} \frac{R_w^*}{(R_w^* + r_L)^2}. \quad (17)$$

Splitting the resistances into mean values and fluctuations, $R_w = \bar{R}_w + r'_w$, $R_w^* = \bar{R}_w^* + r_w'^*$, and assuming that $r'_w \ll \bar{R}_w$ and $r_w'^* \ll \bar{R}_w^*$, Eq. (17) can be linearized. After simplification we obtain $\bar{R}_w = \bar{R}_w^*$, $\bar{I}_w = \bar{I}_w^*$. The first-order differential equation for the resistance fluctuations is then

$$\begin{aligned} & \left[\frac{1}{R_a \bar{I}_w^2} \frac{m_w c_w}{R_a \chi} \frac{(\bar{R}_w - R_a)}{R_a} \frac{1 + \frac{r_L}{\bar{R}_w}}{1 + \frac{R_a r_L}{\bar{R}_w(2\bar{R}_w - R_a)}} \right] \frac{dr'_w}{dt} \\ & + r'_w = r_w'^*. \end{aligned} \quad (18)$$

The apparent time constant of the hot wire in the presence of the connecting lead, noted \tilde{M}_w^{CVA} , is the coefficient multiplying dr'_w/dt and it can be rewritten, using the time constant of the hot wire alone,¹³ noted M_w^{CVA} , as

$$\begin{aligned} \tilde{M}_w^{\text{CVA}} & (\text{with cable resistance } r_L) \\ &= LM \cdot M_w^{\text{CVA}}(\text{hot wire alone}) \end{aligned} \quad (19)$$

with

$$LM = \frac{1 + \frac{r_L}{R_a(1 + \bar{a}_w)}}{1 + \frac{r_L}{R_a(1 + \bar{a}_w)(1 + 2\bar{a}_w)}}. \quad (20)$$

Figure 3 illustrates the variation of LM with r_L/R_a , for several values of \bar{a}_w . The correction factor LM is always larger than unity, unlike LS . For example, $LM \approx 1.08$ for $r_L/R_a \approx 0.25$ and $\bar{a}_w \approx 1$.

In practice, the time constant is measured *in situ* with the lead resistance using the square-wave technique developed by Sarma.² The output of the square-wave test therefore gives \tilde{M}_w^{CVA} . On the other hand, fluctuating quantities in the flow must be obtained using a digital postprocessing tech-

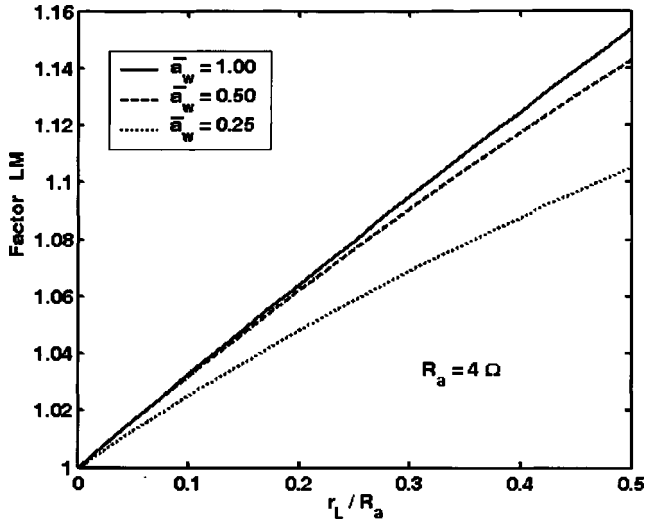


FIG. 3. Effect of the lead resistance r_L on *in situ* measured hot-wire time constants. Factor LM is given by Eq. (20). Three hot-wire overheats \bar{a}_w are considered, and the cold wire resistance is $R_a = 4 \Omega$.

nique that requires the value of the true time constant M_w^{CVA} . For example, at high frequencies, the corrected wire fluctuating signal is given by the simple asymptotic relation⁸

$$e'_{\text{corr}} = \frac{M_w^{CVA}}{TC} e'_{\text{raw}}, \quad (21)$$

where e'_{raw} is the fluctuating signal partially compensated by TC , and e'_{corr} the fully compensated signal. In terms of the CVA output signals and \tilde{M}_w^{CVA} , Eq. (21) can be rewritten as

$$e'_{\text{corr}} = \frac{\tilde{M}_w^{CVA}}{LM \cdot TC} e'_{\text{raw}} \quad (22)$$

which takes into account the effect of the lead resistance.

IV. VALIDATION TESTS

A. Experimental procedure

Validation tests were performed with a $4 \mu\text{m}$ platinum wire (Wollaston type), whose resistance was $R_a = 4.3 \Omega$ at ambient temperature (300 K). The wire is approximately 1.5 mm long, giving an aspect ratio of about 300. The smallest resistance lead used to connect the wire to the CVA was that of a commercial connector (Dantec) with 0.50Ω . For the effect of r_L on LS , three carbon resistances, of 1.0, 2.0, and 3.0Ω , were added one at a time to this cable so that the lead resistance values were: $r_L = 0.50, 1.50, 2.50$, and 3.50Ω . For the effect of r_L on LM , which is the most original part of this investigation, a fourth carbon resistance of 4Ω was also used, so that r_L could attain 4.50Ω . High values of r_L relative to R_a were intentionally chosen, as r_L is the parameter to be studied. Indeed in usual hot-wire anemometry, r_L stays around 1–1.5 Ω . The CVA circuit is the CV01 prototype made by Tao Systems Inc.

For the velocity calibration tests, the hot wire was placed in the potential core of a two-dimensional jet, the mean wire overheat was adjusted to be $\bar{a}_w \approx 0.80$ at all cable resistances, at a mean speed of $\bar{U} = 7.7 \text{ m/s}$. This was done using the fine

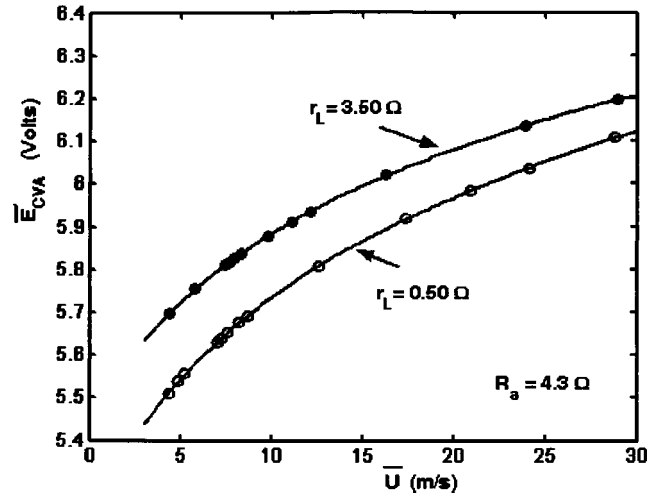


FIG. 4. Calibration curves of the CVA when the lead resistances are $r_L = 0.50 \Omega$ and $r_L = 3.50 \Omega$. The hot-wire overheat is set to $\bar{a}_w \approx 0.80$ at $\bar{U} = 7.7 \text{ m/s}$, for both cable resistances. The cold wire resistance is $R_a = 4.3 \Omega$.

V_w adjustment provided by the CVA unit and the accurate expression which relates $\bar{R}_w + r_L$ to V_w and \bar{V}_s , according to Eq. (1):

$$\bar{R}_w + r_L = \frac{100}{\frac{\bar{V}_s}{V_w} - 1.249}. \quad (23)$$

The velocity (measured by a Pitot tube) was then changed, and the mean output voltage of the CVA, \bar{V}_s , was acquired, using an Agilent 34401A multimeter.

For turbulence measurements, the wire was placed at 65 jet widths downstream of the jet nozzle, on the center of the middle plane. The fan speed was adjusted to provide a mean speed of $\bar{U} = 7.7 \text{ m/s}$ at that location, and $\bar{a}_w \approx 0.80$ was again set at all cable resistances. On the CVA, the time constant was set at $TC = 0.098 \text{ ms}$. The signals were recorded with a 13 bit Hewlett Packard HP 65665A. The sampling frequency was deliberately fixed at a low value, $f_s = 256 \text{ Hz}$, to obtain long recording times, around 8 s. The accuracy on the rms values was estimated to be $\pm 2\%$ when ten records were averaged. The very sharp anti-aliasing filter included in the HP 65665A analyzer, -72 dB per octave, was used.

For the time-constant measurements, the hot wire was again placed in the potential core of the jet. The mean speed was set at 7.7 m/s and the wire overheat at about $\bar{a}_w \approx 0.82$ at all cable resistances. The square-wave test system incorporated in the CVA was used. The 63% decay and rise times of the square wave were measured with a HP 54645D numerical oscilloscope equipped with a mega zoom. The very low turbulence level in the potential core permitted accurate and fast measurements of \tilde{M}_w^{CVA} , within about $\pm 5 \mu\text{s}$.

B. Results for the LS sensitivity factor

The calibration curves obtained in the two extreme cases of $r_L = 0.50 \Omega$ and $r_L = 3.5 \Omega$ are presented in Fig. 4. The cable has a clear effect of shifting the curve upward and of reducing its slope at all mean velocities. However, the value

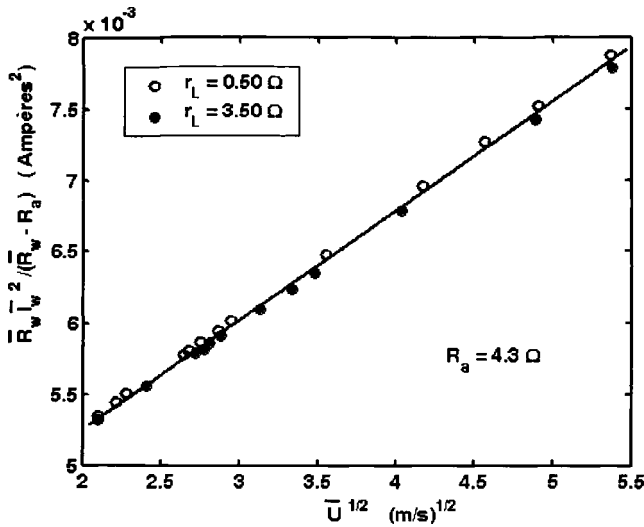


FIG. 5. Heat transfer law of the hot wire (King’s law), deduced from the two curves of Fig. 4.

of $\bar{R}_w^{-1/2} / (\bar{R}_w - R_a)$, even with the lead resistances, follows, as it should, a unique straight line curve with $U^{0.5}$, expressing King’s law for the wire itself, independent of the anemometer as illustrated in Fig. 5.

Table I gives the summary of the test conditions and turbulence values, with or without the *LS* factor included. The last column clearly indicates that the same values of u'/\bar{U} are recovered when the *LS* correction is applied.

Here, the u'/\bar{U} values concern the resolved bandwidth of the HP 65665A, up to $f = f_s/2 = 128$ Hz and they deal with raw data^{3,8} collected with the CVA internal compensation set at $TC = 0.098$ ms. In the present case, measured M_w^{CVA} is of the order of 0.20 ms, as we will see in Sec. IV B, and for frequencies less than 128 Hz, the M_w^{CVA} software correction is negligible, at maximum it would be $[1 + (2\pi f M_w^{CVA})^2] \approx 1.02$ for $f = 128$ Hz.

In these experiments \bar{U} and \bar{a}_w were always set at the same value. This improved the accuracy of the measurements by keeping strictly constant the King’s law coefficients *A* and *B* and all the parasitic thermal leaks, in particular those towards the wire supports.^{18,19}

C. Results for the LM time-constant factor

Figure 6 shows the values obtained for the time constant with different lead resistances r_L . Both the 63% decay and rise times of the square have been reported. A clear increase of both values is observed with r_L .

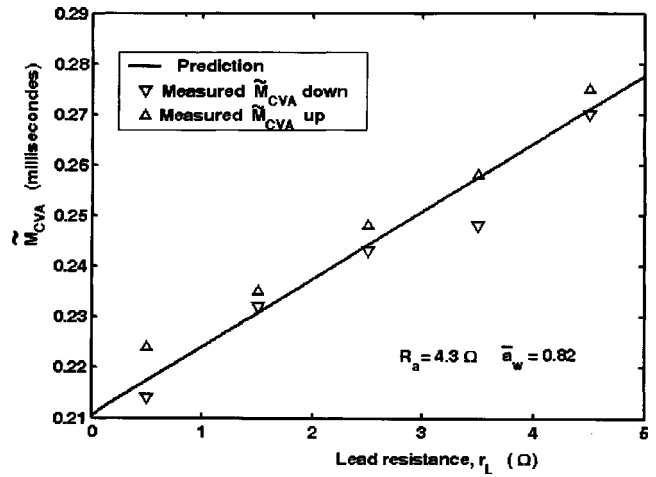


FIG. 6. Effect of the lead resistance r_L on the hot-wire time constant measured *in situ* by the square-wave test technique: \tilde{M}_{CVA}^{down} is the 63% point on the decaying signal and \tilde{M}_{CVA}^{up} is the 63% point on the rising signal. The hot-wire overheat is set to $\bar{a}_w \approx 0.82$ at $\bar{U} = 7.7$ m/s for all cable resistances. The line corresponds to Eqs. (19) and (20).

The straight line drawn in Fig. 6 corresponds to expressions (19) and (20) which give $M_w^{CVA} = LM \cdot M_w^{CVA}$. For the M_w^{CVA} value of the wire alone the following expression⁸ was used:

$$M_w^{CVA} = \frac{1 + \bar{a}_w}{1 + 2\bar{a}_w} \frac{d^2}{4} \frac{\rho_w c_w}{k_a} \frac{1}{A' + B' \sqrt{Re_d}}, \tag{24}$$

where $A' = 0.24$ and $B' = 0.56$ are the constants of the forced convection heat transfer of the wire when expressed in terms of Nusselt and Reynolds numbers.^{17,18} For platinum $\rho_w = 21\,450$ kg m⁻³ and $c_w = 130$ J kg⁻¹ K⁻¹, and for air at 300 K the thermal conductivity is $k_a = 0.02624$ W m⁻¹ K⁻¹. The wire diameter is approximated by 3.6 μ m to allow a translation of the line parallel to the ordinates, the slope being unchanged. $Re_d \approx 2$ is the wire Reynolds number at 7.7 m/s. The line which expresses \tilde{M}_w^{CVA} versus the cable resistance r_L agrees very well with the measured results.

Table II gives a summary of the test conditions and measured values of \tilde{M}_w^{CVA} for different lead resistances. The last column clearly indicates that M_w^{CVA} (wire alone) is very well estimated with the *LM* factor. The high values deliberately chosen for r_L show that expression (20) can be used with confidence, although in practical measurements only smaller r_L are generally encountered.

TABLE I. Summary of CVA test conditions for turbulence measurements in a subsonic jet, $R_a = 4.3 \Omega$.

r_L Ohms	V_w Volts	\bar{a}_w	e'_{CVA} Volts	\bar{E}_{CVA} Volts	u'/\bar{U} % without <i>LS</i> included	<i>LS</i>	u'/\bar{U} % with <i>LS</i> included
0.50	0.424	0.78	0.081	5.722	25.11	0.8795	28.55
1.50	0.480	0.80	0.0765	5.790	23.21	0.8286	28.01
2.50	0.529	0.79	0.073	5.834	22.09	0.7819	28.25
3.50	0.582	0.79	0.070	5.925	20.85	0.7397	28.19

TABLE II. Summary of CVA test conditions for time-constant measurements in a subsonic jet, $R_a=4.3 \Omega$.

r_L Ohms	V_w Volts	V_s Volts	\bar{a}_w	Measured \bar{M}_w^{CVA} down ms	Measured \bar{M}_w^{CVA} up ms	LM	\bar{M}_w^{CVA} (mean) corrected by LM , ms
0.50	0.4385	5.761	0.84	0.214	0.224	1.038	0.211
1.50	0.4799	5.725	0.83	0.232	0.235	1.111	0.210
2.50	0.5290	5.778	0.82	0.243	0.248	1.177	0.209
3.50	0.5925	5.916	0.85	0.248	0.258	1.237	0.205
4.50	0.6360	5.923	0.84	0.270	0.275	1.292	0.211

V. SUPERSONIC TURBULENCE MEASUREMENTS

The procedure described above was also applied to tests with CVA in a Mach 2.54 supersonic boundary layer in the HMMS wind tunnel of the IAG Institute at the University of Stuttgart. All experimental parameters have been reported by Weiss *et al.*⁹ Data from tests at $y/\delta=0.36$, where y is the distance from the wall and δ , the boundary layer thickness, was used here. A 5 μm tungsten wire was used in that investigation; its cold resistance was $R_a=3.0 \Omega$. The cable resistance was constituted by the resistance of the prongs and its short connecting Dantec cable, 0.5 Ω , and the resistance of a Dantec 5-m-long cable, 0.7 Ω , hence $r_L=1.2 \Omega$. Experiments were done with the same VC01 CVA prototype as described in Sec. IV. Data from 12 wire overheats were used to enable the estimation of mass flux and total temperature fluctuations in the turbulent supersonic flow. At each \bar{a}_w , the \bar{M}_w^{CVA} values were measured with the usual square wave technique. In the data processing previously presented,⁹ however, the CVA response was only partially corrected by the LS factor—represented by “Q” in Ref. 9.

If we take into account both the LS and the LM factors, the parabola which expresses

$$K = \frac{\overline{e_{CVA}^{\prime 2}}}{(\overline{E_{CVA}})^2} (1 + 2\bar{a}_w)^2 \tag{25}$$

has the form

$$K_{corr} = \frac{1}{(LS)^2(LM)^2} \left[\frac{\overline{e_{CVA}^{\prime 2}}}{\overline{E_{CVA}}^2} (1 + 2\bar{a}_w)^2 \right] = \left[\frac{\bar{a}_w^2}{4} T_{\rho u}^2 - \bar{a}_w R + T_{\theta_t}^2 \right]. \tag{26}$$

The right-hand side of expression (26) is fixed by the turbulence: $T_{\rho u}$ and T_{θ_t} are the turbulence mass flux and total temperature levels and R is the correlation coefficient between the corresponding fluctuations.

Figure 7 shows the experimental data obtained for the left-hand side of expression (26) as a function of the wire overheat \bar{a}_w . Curve K_0 shows the uncorrected data. When both the LS and LM corrections are applied, curve K_2 is obtained. The separate effects of LS and LM can easily be deduced from Table III which indicates the LS and LM values for this experimental case ($R_a=3 \Omega$, $r_L=1.2 \Omega$). Two major conclusions can be noted:

- (1) Interestingly, the K_0 curve is quite close to the K_2 curve, which means that “no correction at all” could be a valuable simplified approach.
- (2) Table III shows that this is particularly exact at high overheats, the product of $LS.LM$ approaching one. At lower overheats, around $\bar{a}_w \leq 0.40$, the LS and LM corrections are in principle needed. In the present experiments they affect slightly the T_{θ_t} measurements because the total temperature fluctuations are small in a supersonic turbulent boundary. The coefficients of expression (26), obtained by fitting a parabola to the experimental data, indeed give $T_{\rho u}=7.2\%$, $T_{\theta_t}=2.4\%$, and $R=0.0014$ for curve K_2 , and $T_{\rho u}=7.0\%$, $T_{\theta_t}=1.7\%$, and $R=0.0011$ for curve K_0 . As expected the T_{θ_t} value is slightly larger for curve K_2 .

Data collected with a CTA system in the same test are also presented in Fig. 7. The J expression which corresponds to K has the advantage of being independent of the lead resistance¹⁴

$$J = 4\bar{a}_w^2 \left[\frac{e_{CTA}^{\prime 2}}{\overline{E_{CTA}}^2} \right] = \left[\frac{\bar{a}_w^2}{4} T_{\rho u}^2 - \bar{a}_w R + T_{\theta_t}^2 \right], \tag{27}$$

but to achieve a sufficiently high frequency response, comparable to that of the CVA, a specific transfer function has to be acquired ahead of time for every overheat \bar{a}_w and also at a known offset applied to the feedback amplifier.^{20,21} These

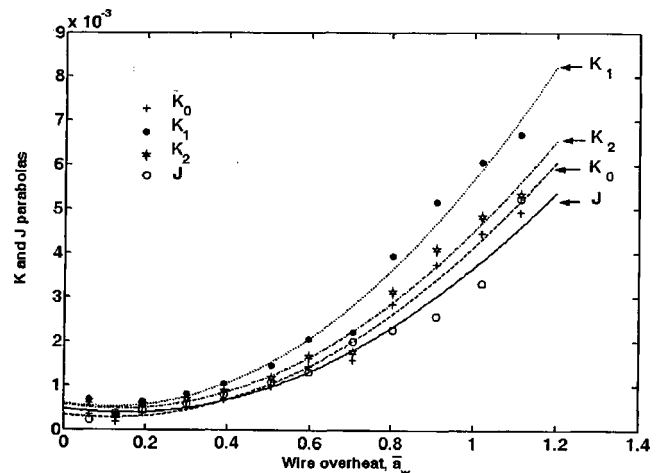


FIG. 7. Turbulence data obtained in a Mach 2.54 boundary layer at different hot-wire overheats \bar{a}_w . For CVA, K is defined by Eq. (26), K_0 is without correction ($LS=LM=1$), K_1 includes only the LS correction, K_2 includes both the LS and LM corrections. For the CTA, J is defined by Eq. (27).

TABLE III. LS and LM factors for experiments in a supersonic boundary layer, $R_a=3 \Omega$, $r_L=1.2 \Omega$.

\bar{a}_w	0.10	0.20	0.30	0.50	0.70	0.90	1.10
LS	0.724	0.759	0.785	0.820	0.840	0.852	0.858
LM	1.046	1.077	1.097	1.118	1.125	1.126	1.124
$LS.LM$	0.758	0.817	0.861	0.916	0.945	0.959	0.964

independent measurements give for the turbulence parameters: $T_{\rho u}=6.7\%$, $T_{\theta_t}=2.2\%$, and $R=0.0013$. Within the experimental errors one can conclude that a good agreement exists between the fully corrected CVA and the fully corrected CTA results.

Finally, in the CVA data previously reported,⁹ only the LS correction was used. This partial correction yields curve K_1 which is well above the other curves, as reported in Fig. 7. As a consequence, the turbulence levels are much too large. Indeed, a parabola fit to K_1 gives $T_{\rho u}=8.0\%$, $T_{\theta_t}=2.5\%$, and $R=0.0015$.

VI. DISCUSSION

It has been established through analysis and experiments that the outputs measured from the CVA need to be corrected for the cable lead resistance for improved accuracy, but such corrections rely on easily measurable parameters.

Due to the nature of the variations it was shown that the errors from the lead resistance on the sensitivity coefficient (LS) and time constant (LM) tend to offer some cancellation of the net effect due to the lead resistance.

It should be noted that even if the static sensitivity coefficients are obtained by direct calibrations, the effect of the lead resistance has to be taken into account in the determination of the wire time constant. Otherwise, the turbulent quantities can be overestimated.

ACKNOWLEDGMENTS

The authors are indebted to Professor Dr.-Ing. Siegfried Wagner and Dr.-Ing. Helmut Knauss for allowing measurements in the supersonic wind tunnel of IAG. They express

many thanks to Dr. Siva M. Mangalam and Dr. Garimella R. Sarma from Tao Systems Inc. who permitted the use of a recent CVA prototype. They are also very grateful to Dr. Garimella R. Sarma for his stimulating discussions and constructive views.

¹G. R. Sarma, U.S. Patent No. 5,074,147 (1991).

²G. R. Sarma, Rev. Sci. Instrum. **69**, 2385 (1998).

³G. R. Sarma, G. Comte-Bellot, and T. Faure, Rev. Sci. Instrum. **69**, 3223 (1998).

⁴G. R. Sarma and R. W. Lankes, Rev. Sci. Instrum. **70**, 2384 (1999).

⁵G. R. Sarma and G. Comte-Bellot, Rev. Sci. Instrum. **73**, 1313 (2002).

⁶R. E. Drubka, J. Tan-Artichat, and H. M. Nagib, DISA Inf. **22**, 5 (1977).

⁷G. E. Truzzi, G. R. Sarma, and N. Chokani, Rev. Sci. Instrum. **73**, 4363 (2002).

⁸G. Comte-Bellot and G. R. Sarma, AIAA J. **39**, 261 (2001).

⁹J. Weiss, H. Knauss, S. Wagner, N. Chokani, G. Comte-Bellot, and A. D. Kosinov, AIAA Paper 2003-1277, 41st AIAA Aerospace Sciences Meeting & Exhibit, Reno, NV, 6–9 January 2003.

¹⁰J. T. Lachowicz, N. Chokani, and S. P. Wilkinson, AIAA Paper 96-0782, 34th Aerospace Sciences Meeting & Exhibit, Reno, NV, 15–18 January 1996.

¹¹C. A. Reimann, N. Chokani, and G. R. Sarma, in Ref. 9, AIAA Paper 2003-0976.

¹²J. D. Norris and C. Chokani, AIAA J. **41**, 1619 (2003).

¹³G. Comte-Bellot, in *Handbook of Fluid Dynamics*, edited by R. W. Johnson (CRC, Boca Raton, FL, 1998), Chap. 34.

¹⁴C. Bailly and G. Comte-Bellot, *Turbulence* (CNRS, Paris, 2003).

¹⁵A. E. Blanchard, J. T. Lachowicz, and S. P. Wilkinson, AIAA J. **35**, 23 (1997).

¹⁶H. Ito, G. E. Truzzi, G. R. Sarma, and N. Chokani, in Ref. 9, AIAA Paper 2003-1293.

¹⁷H. H. Bruun, *Hot-Wire Anemometry, Principles and Signal Analysis* (Oxford University Press, Oxford, 1995).

¹⁸S. Corrsin, in *Handbuch der Physik, Encyclopedia of Physics*, edited by S. Flügge (Springer, Berlin, 1963), Vol. VIII/2, p. 524.

¹⁹S. C. Morris and J. F. Foss, Meas. Sci. Technol. **14**, 251 (2003).

²⁰J. Weiss, H. Knauss, and S. Wagner, Rev. Sci. Instrum. **72**, 1904 (2001).

²¹J. Weiss, Meas. Sci. Technol. **14**, 1373 (2003).